ACS APPLIED MATERIALS & INTERFACES

Research Article

www.acsami.org

Small GSH-Capped $CuInS_2$ Quantum Dots: MPA-Assisted Aqueous Phase Transfer and Bioimaging Applications

Chuanzhen Zhao,[†,∥] Zelong Bai,[†,∥] Xiangyou Liu,[‡] Yijia Zhang,[†] Bingsuo Zou,[§] and Haizheng Zhong*[,†]

[†]Beijing Key Laboratory of Nanophotonics and Ultrafine Optoelectronic Systems, School of Materials Science & Engineering, Beijing Institute of Technology, 5 Zhongguancun South Street, Beijing 100081, P. R. China

[‡]Cancer Research Center, Sanford-Burnham Medical Research Institute, La Jolla, California 92037, United States

[§]Micro Nano Technology Center, Beijing Institute of Technology, 5 Zhongguancun South Street, Beijing 100081, P. R. China

Supporting Information

ABSTRACT: An efficient ligand exchange strategy for aqueous phase transfer of hydrophobic $CuInS_2$/ZnS quantum dots was developed by employing glutathione (GSH) and mercaptopropionic acid (MPA) as the ligands. The whole process takes less than 20 min and can be scaled up to gram amount. The material characterizations show that the final aqueous soluble samples are solely capped with GSH on the surface. Importantly, these GSH-capped $CuInS_2$/ZnS quantum dots have small size (hydrodynamic diameter <10 nm), moderate fluorescent properties (up to 34%) as well as high stability in aqueous solutions (stable for more than three months in 4 °C without any significant fluorescence quenching). Moreover, this ligand exchange strategy is also versatile for the aqueous phase transfer of other hydrophobic quantum dots, for instance, $CuInSe_2$ and CdSe/ZnS quantum dots. We further demonstrated that GSH-capped quantum dots could be suitable fluorescence markers to penetrate cell membrane and image the cells. In addition, the GSH-capped $CuInS_2$ quantum dots also have potential use in other fields such as photocatalysis and quantum dots sensitized solar cells.

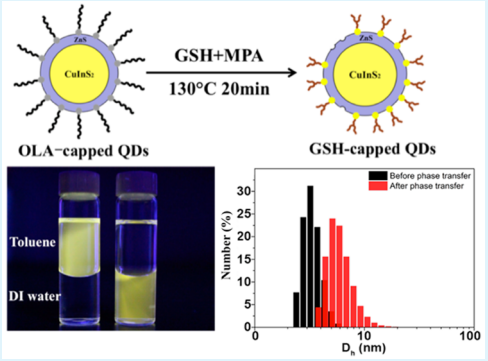

KEYWORDS: *quantum dots, semiconductor nanocrystals, aqueous phase transfer, ligand exchange, glutathione*

1. INTRODUCTION

Semiconductor nanocrystals (NCs), also known as quantum dots (QDs), are very attractive fluorescent markers for biological probes and imaging applications due to their small particle size, enhanced photostability, broad emission tunability, and high extinction coefficient.[1−5] Unfortunately, most of the highly luminescent QDs currently used for bioimaging are composed of class A toxic elements (Cd, Hg, Pb, Se, Te, etc.).[6−11] The cytotoxicity of these QDs has been a great challenge for developing in vivo biotechniques.[12,13] On the contrary, I−III−VI $CuInS_2$ and $CuInSe_2$ QDs have a large spectral tunable range (500−900 nm) and high photoluminescence quantum yields (PLQYs ≈ 70%) and less toxicity, which make them promising candidates for bioapplicaitons.[14−20] Although, $CuInS_2$ based QDs could be directly fabricated in water, the available aqueous routes only give samples with narrow emissive ranges and low QYs.[21−23] High-quality I−III−VI $CuInS_2$ and $CuInSe_2$ QDs produced in organic solvents are insoluble in water.[24−27] Hence a current challenge is to achieve efficient phase transfer of hydrophobic $CuInS_2$ and $CuInSe_2$ based QDs into aqueous solution with keeping good fluorescent properties.[28−34]

There are three commonly used aqueous phase transfer strategies, including ligand exchange, forming micelle through hydrophobic interaction, and silica (or polymer) encapsulation.[35] Among them, ligand exchange is one of the widespread used aqueous phase transfer strategies.[36−38] The other two strategies usually increase the particle size to dozens or even hundreds nanometers,[39−41] whereas ligand exchange strategy can perfectly maintain the small particle size and monodispersity of QDs, which is crucial for either in vitro or in vivo bioimaging applications, especially in cellular imaging, protein (or DNA, virus) tracing, and so on.[42−44] Mercaptopropionic acid (MPA) is the most commonly used ligand in aqueous phase transfer strategies. However, due to its high activity to form disulfide, the prepared QDs in aqueous solution will aggregate and precipitate out of water in a short time, which is unacceptable in most bioimaging applications.[45] Although many other ligands (DHLA, PEG-SH, etc.) can provide QDs a better performance in solubility and stability, the affordable prices and low production rates still hinder the popular utilization of these strategies.[46−49] Glutathione (GSH), as a common biological molecular, has appropriate price. It also can provide high-quality water-solubility and good biocompatibility as well as chiral response when capping QDs.[50,51] Since 2004, Vogel et al.[52] first reported the aqueous synthesis of GSH-

Received: January 23, 2015
Accepted: July 27, 2015
Published: July 27, 2015

DOI: 10.1021/acsami.5b05503
ACS Appl. Mater. Interfaces 2015, 7, 17623−17629

capped CdSe QDs, many in situ synthesis strategies of GSH-capped II−VI QDs were developed subsequently.[53−55] In comparison to the in situ synthesis, only limited strategy is available for effective phase transfer of hydrophobic QDs, especially I−III−VI $CuInS_2$ and $CuInSe_2$ based QDs, into aqueous solution using GSH as ligands.

Recently, we developed the colloidal chemistry of non-injection technique to synthesize highly luminescent I−III−VI $CuInS_2$ and $CuInSe_2$ based QDs in organic phase.[24,56−58] The availability of these high quality materials at gram amount provides the opportunity to explore their potential in various applications.[14] Herein, we report a facile strategy to transfer $CuInS_2$/ZnS core/shell QDs from the organic to aqueous solvent with high transfer efficiency and effective preservation of the PLQY using MPA and GSH as ligands. With this method, we achieved high-quality hydrophilic $CuInS_2$/ZnS QDs with PLQY over 30%, small particle size less than 10 nm, and good monodispersity. The GSH ligands also enable QDs good biocompatibility and a colloidal stability over three months at 4 °C. All these features make GSH-capped $CuInS_2$/ZnS QDs suitable material for various applications. It is also noteworthy that the ligand exchange process can be finished within 20 min, as well as scaled up to gram amounts.

2. EXPERIMENTAL SECTION

2.1. Chemicals. Copper(I) iodide (CuI, Alfa Aesar, 98%), indium(III) acetate ($In(OAc)_3$, Alfa Aesar, 99.99%), zinc acetate ($Zn(OAc)_2$, Alfa Aesar, ≥97%), 1-dodecanethiol (DDT, Alfa Aesar, 98%), 1-octadecene (ODE, Alfa Aesar, 90%), oleic acid (OA, Alfa Aesar, 90%), oleylamine (OLA, J&K Scientific, 90%), *N*,*N*-dimethylformamide (DMF, Alfa Aesar, 99.7+%), 3-mercaptopropionic acid (MPA, TCI development Co., Ltd., > 98%), and L-glutathione (GSH, Aladdin, 98%) were used.

2.2. Synthesis of $CuInS_2$/ZnS NCs. The $CuInS_2$/ZnS QDs were prepared in ODE and purified as described in our previous reports and the details are shown as follow. CuI (0.038 g, 0.2 mmol), $Zn(OAc)_2$ (0.088 g, 0.5 mmol) and $In(OAc)_3$ (0.232 g, 0.8 mmol) were mixed with 2 mL DDT and 4 mL ODE. The reaction mixture was degassed under vacuum for 20 min at 120 °C. After that, 1 mL OA was added into the reaction flask. The solution was then heated to 230 °C for 30 min until a colloidal solution was formed with the protection of nitrogen. Zinc stock solution was first prepared as follows. The mixture of $Zn(OAc)_2$ (0.528 g, 3 mmol), 2 mL of OLA, and 2 mL of ODE was degassed for 30 min. Next, the solution was heated to 130 °C until a clear colorless solution was formed with the protection of nitrogen. The obtained Zn stock solution was maintained at this stage for following injection. Subsequently, 4 mL Zn stock solution was added dropwise into the reaction mixture. Afterward, the reaction solution was cooled to room temperature and precipitated by adding excess acetone. The flocculent precipitate was centrifuged at 7000 rpm for 3 min and the supernatant decanted. This process was repeated a minimum of three times, and the precipitation was then dispersed in a nonpolar solvent (toluene, chloroform) or dried to powder.

2.3. Aqueous Phase Transfer Using GSH and MPA. The aqueous phase transfer was achieved by replacing the initial surface ligands using GSH and MPA as coligands, as shown in the following steps. A mixture of MPA (2 mL, ∼20 mmol), GSH (230 mg, 0.75 mmol), and 100 mg $CuInS_2$/ZnS QDs powder were added into 3 mL of *N*,*N*-dimethylformamide (DMF) and formed a turbid solution. Then, the mixture was heated to 130 °C and stirred with the protection of nitrogen. After 10−15 min, the mixture solution became clear gradually. Finally, the product was precipitated by adding 10 mL of methanol or 2-propanol and centrifugated at 6000 rpm for 3 min. The precipitates were dissolved in alkaline buffer solution (pH ∼10) to store. The transfer yields are usually over 50% in weight.

2.4. Characterization. Absorption spectra were recorded on a V-570 UV−vis spectrophotometer. PL spectra were taken using a FP-6600 luminescence spectrometer. The PLQYs of samples were measured by using rhodamine B as a standard reference (rhodamine B dissolved in ethanol, QY: 97%) and comparing integrated PL intensities using the standard procedure.[59] The PL emission of rhodamine B was measured with excitation wavelength at 520 nm. The PLQYs of QDs was calculated as

$$QY = QY_R \frac{I}{I_R} \frac{A_R}{A} \frac{n^2}{n_R^2}$$

where QY is the quantum yield of samples, I is the measured integrated PL emission intensity, n is the refractive index of solvent (n = 1.497 for toluene; n = 1.33 for deionized water; n = 1.42 for DMF), and A is the optical density at the excitation wavelength (A is typically around 0.05). The subscript R refers to the parameters of the reference. All the $CuInS_2$/ZnS NCs samples were measured using an FP-6600 spectrophotometer with excitation wavelength at 420 nm. TEM and HRTEM images were taken on a JEM-2100F transmission electron microscope with an acceleration voltage of 200 kV. ^1H NMR spectra were recorded on a Varian mercury-plus 400 spectrometer. Fourier transform infrared (FT-IR) spectra were recorded on an IRPrestige-21 spectrophotometer. Dynamic light scattering (DLS) measurement and zeta potential were carried out on Malvern Nano-ZS Zetasizer Nano series.

2.5. Bioimaging Experiments. Cytotoxicity assay was performed according to the procedures described previously.[60] Briefly, the cells were seeded into a 96-well plate (Corning, U.S.A.) and grown to a density of 104 cells per well. Then serial dilutions of the QDs samples were added and coincubated with the cells for 48 h. Subsequently, CCK-8 solution (20 mL/well) was added and the plate was further incubated for 30 min. The absorbance of each well at 450 nm was determined using FlexStation 3 multimode microplate reader (Molecular Devices). For bioimaging, $CuInS_2$/ZnS QDs were incubated with MCF10CA1a cells in Petri dish for 30 min at 37 °C incubator, followed by washing with PBS three times, staining with Hoechst 33342 for 20 min, and washing again. The cells were finally observed with a Zeiss LSM710 confocal microscope.

3. RESULTS AND DISCUSSION

Figure 1a illustrates the aqueous phase transfer strategy. Briefly, hydrophobic $CuInS_2$/ZnS QDs were synthesized according to

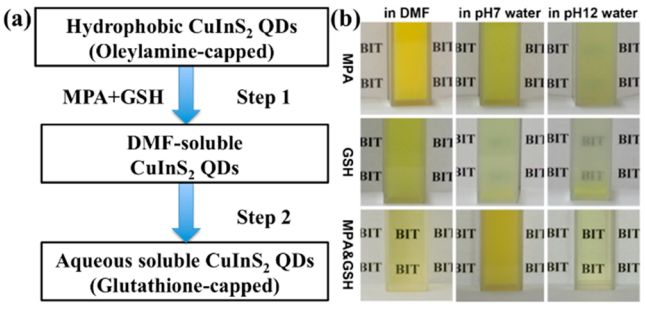

Figure 1. (a) Schematic presentation of the phase transfer route. (b) Photographs of samples treated with different surface ligands (left) dissolved in different solvents (top).

our previous reports.[24] A fixed amount of the as-prepared samples were dissolved into DMF with a mixture of GSH and MPA at 130 °C under vigorous string (Step 1). The samples were then precipitated from DMF with adding methanol and redispersed into water or buffer solution (pH 12) to form aqueous soluble $CuInS_2$/ZnS QDs. To investigate the mechanism of ligand exchange and optimize the phase transfer, parallel experiments were carried out using MPA and GSH respectively as ligands in the reaction system under the same circumstance. Because the solubility of QDs strongly depends

DOI: 10.1021/acsami.5b05503
ACS Appl. Mater. Interfaces 2015, 7, 17623−17629

on their surface ligands, the successful phase transfer of these samples after ligand exchange can be directly demonstrated by the transparency of the resulting solutions. Figure 1b show the optical images of the resulting samples in DMF or in water at pH 7 and 12, respectively. It is observed that the samples after ligand exchange using MPA or GSH respectively give opaque suspensions. Only the QDs after ligand exchange with a combination of GSH and MPA are soluble in DMF. Moreover, the $CuInS_2$ based QDs precipitated from DMF are insoluble in neutral solution (pH 7) but become soluable after neutralization with alkaline water solution (pH 10−12). We further stuided the variation of PLQY and zeta potential of resulting samples with the ratio of GSH and MPA (see Table S1 in the Supooring Information). An optimized molar ratio of GSH and MPA at 1:1 gives the highest PLQY of ∼34%. These phenomena imply that the combination of these two ligands have a significant effect in the ligand exchange process. Moreover, the MPA assisted ligand exchange strategy using GSH can be further extended to the aqueous phase transfer of other hydrophobic quantum dots, for instance, $CuInSe_2$ and CdSe/ZnS quantum dots (see Figure S1 in the Supooring Information). It is worth noting that the ligand exchange can be simply scaled up to obtain gram scale aqueous soluble QDs (see Figure S2 in the Supporting Information).

To understand the ligand exchange process, we further analyzed the products by characterizing the final products. Thermogravimetric analysis (TGA) was applied to determine the samples before and after ligand exchange and the results are shown in the Supporting Information (see Figure S3). The obvious reduction of the weight loss suggests the success of ligand exchange. In order to further comprehend the function of GSH and MPA in the ligand exchange process, FTIR and ^1H NMR characterizations were carried out to determine the nature of surface ligands. Figure 2a shows the FTIR spectra of QDs before ligand exchange, after ligand exchange with only MPA, and after ligand exchange with MPA and GSH, respectively. It was found that QDs after ligand exchange have a sharp band at 1698 cm^{-1}, which can be assigned to the carbon−oxygen double bond stretching vibration from MPA or GSH.[48] In contrast, the OLA capped QDs before ligand exchange do not have any signal of carboxyl from GSH and/or MPA. Thus, the FITR spectra provide evidence for the successful ligand exchange on the surface of QDs.

To further confirm the species and ratio of surface ligands, the QDs before and after the ligand exchange process were investigated by 1H-NMR (see Figure 2b). There is a peak at δ 1.25 ppm of QDs before ligand exchange, which can be attributed to the hydrogen at $-CH_2-$ and is a characteristic peak for OLA. Obviously, there's no peak from δ 0 ppm to δ 2 ppm of QDs after the ligand exchange process, indicating that the formal ligands on the surface of OLA-capped QDs have been replaced. Meanwhile, the peaks centered at δ 2.3 ppm, δ 2.55 ppm, and δ 2.9 ppm represent the H atom on methylene in the GSH molecule. In contrast with formal view of partly exchange process, this result provides cogent evidence that the ligands have been replaced completely since there is not any peak of OLA. Meanwhile, compared with the 1H-NMR spectra of GSH, MPA molecular, and QDs after ligand exchange, the missing of peaks between δ 2.6 ppm to δ 2.8 ppm indicates support for the absence of MPA on the surface of $CuInS_2$/ZnS QDs. Based on these results, we supposed the MPA only plays an auxiliary role in the reaction, but does not cover the QD's surface in the final product.

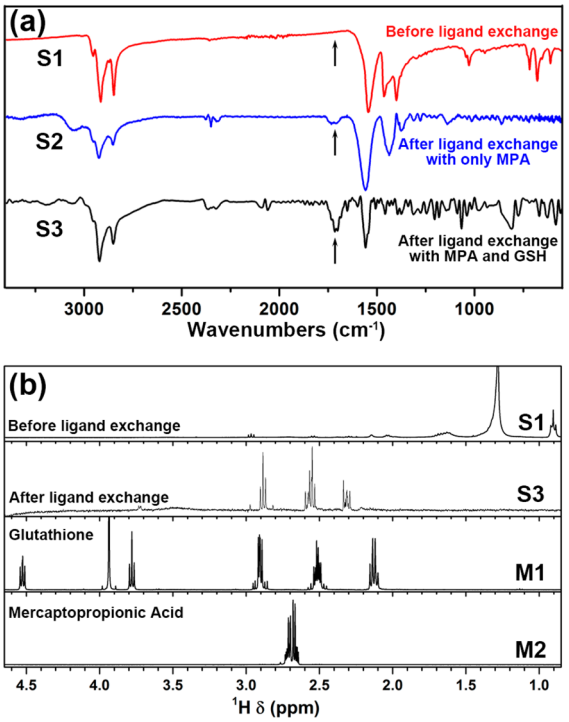

Figure 2. (a) FTIR spectra of OLA capped $CuInS_2$/ZnS QDs before ligand exchange (S1), the sample after ligand exchange with MPA (S2), the sample after ligand exchange using MPA and GSH (S3); (b) 1H-NMR spectra of OLA capped $CuInS_2$/ZnS QDs before ligand exchange (S1) in chloroform-d, the sample after ligand exchange using MPA and GSH (S3) in D_2O, GSH (M1) and MPA (M2) in D_2O.

According to the literature reports, the dynamic of ligand on QDs surface can be described as an adsorption−desorption equilibrium process.[38] Based on the literature and our experimental results, the ligand exchange process can be further explained as follow. As illustrated in Scheme 1, MPA has a high affinity to the QD's surface and is likely to replace the original capping ligand of OLA. In contrast to small lineral structure of MPA, GSH is a tripeptide with linkage between the carboxyl group of the glutamate side-chain and the amine group of cysteine (see Figure S4 in the Supporting Information). Due to possible steric hindrance from GSH, MPA is more likely to replace OLA on the surface to obtain MPA-coated QDs in DMF, although both of MPA and GSH are susceptible to oxidation under disulfide formation.[45,46] Acccording to the literature, the transformation of thiol/disulfide systems is determined by the half-cell potential relative to the stanard hydrogen electrode. GSH has a half cell potential E disulfide/thiol of −0.262 V, which is higher relative to the value of MPA (−0.257 V).[61] Therefore, MPA-coated QDs are prone to be replaced by GSH due to the higher reduction potential for formation disulfide.

As shown in Figure 3a, GSH-capped $CuInS_2$/ZnS QDs can be dissolved in alkaline water. Therefore, the final products after ligand exchange were further characterized by applying difference techniques. Figure 3b shows the results of DLS measurements. It is observed that the hydrodynamic diameters (HDs) of QDs increased slightly from ∼4 to ∼6 nm. The GSH-capped $CuInS_2$/ZnS QDs have zeta potential of −47.5 ± 0.8 mV in deionized water, which is in consistent with the presence of a carboxyl group on their surface. Figure 3c,d presents the TEM images of the QDs before and after ligand exchange. It

DOI: 10.1021/acsami.5b05503
ACS Appl. Mater. Interfaces 2015, 7, 17623−17629

Scheme 1. Illustration of Proposed Mechanism for the Ligand Exchange Process

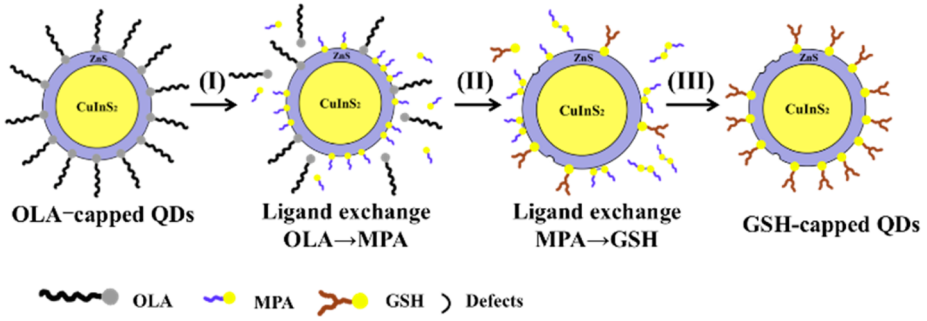

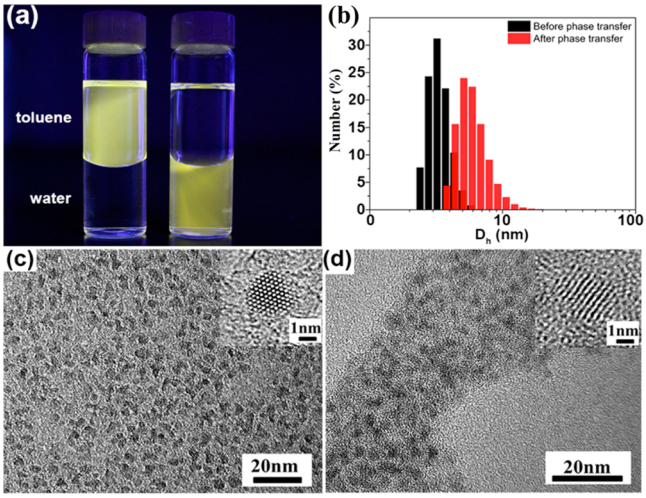

Figure 3. (a) Photographs of samples before and after ligand exchange under UV light; (b) DLS data of $CuInS_2$/ZnS QDs before and after ligand exchange; (c) and (d) are TEM and HRTEM images of $CuInS_2$/ZnS QDs before (c) and after (d) ligand exchange, respectively.

appears that $CuInS_2$/ZnS QDs are well isolated and rarely observed as aggregates. As is shown in HRTEM, the shape and size of QDs in aqueous solution were almost the same as the one in toluene, which provides further evidence that the dispersity and size of QDs were slightly altered during the ligand exchange process.

As we discussed in the introduction, the compact size and favorable dispersibility not only satisfy the request for general biological imaging application but also provide specific application prospect, in brain tumor[62] and nucleus imaging.[6] Figures 4a and S5 show the UV−visible absorption and PL emission spectra of QDs before and after ligand exchange. The fluorescence emission peaks and full width at half maxima (fwhm) for the samples after ligand exchange is almost the same as it before ligand exchange, indicating no obvious change in the particle size and structure. Thus, the QDs retain their photoluminescence properties during the ligand exchange, which is important for phase transfer.[46] To illustrate the advantages of our GSH capped $CuInS_2$ based QDs, we compared the resulting GSH capped QDs with other samples using 11-Mercaptoundecanoic acid (MUA), forming micelle using CTAB[63] and polymer encapsulating using F127. The methods are described in details in the Supporting Information. As illustrated in Figure 4b, our ligand exchange method gives an optimized PLQY of ~34% for $CuInS_2$ based QDs in deionized water. In contrast, the PLQYs of the aqueous QDs that phase

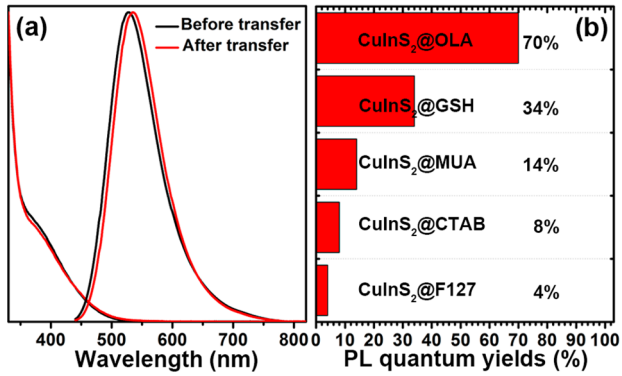

Figure 4. (a) UV and PL spectra of $CuInS_2$/ZnS QDs before and after ligand exchange; (b) QYs of samples with different aqueous phase transfer strategies.

transferred from the same sample using 11-MUA, CTAB and F127 are 14%, 8%, and 4%, respectively, which confirm the advantage of a combination of GSH and MPA in the ligand exchange process.

The colloidal stability of hydrophilic QDs in the aqueous solution is very important for their bioimaging applications.[64−66] We further conducted the stability test under various conditions. Within the experimental limits, during more than three months, nearly no decrease of PLQY was observed, which is rare for QDs transferred by ligand exchange and with PLQY over 30% (Figure 5a). Comparative analysis was also

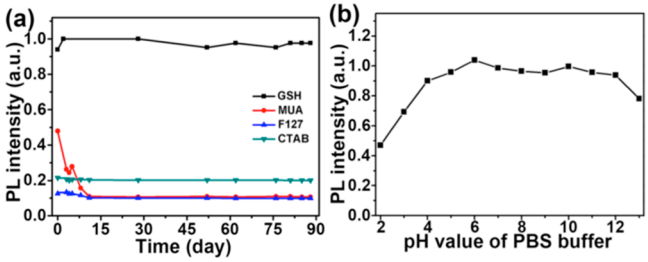

Figure 5. (a) Stability of samples with different surface modification methods; (b) pH resistance of GSH-capped $CuInS_2$/ZnS QDs.

carried out between QDs transferred through other methods. The results show that QDs transferred by MUA, which also belonged to ligand exchange strategy, behaved a poor stability after 10 days. Although the QDs transferred by CTAB and F127 exhibit a high stability, but suffering from the low PLQYs. In some application, especially sensor and detection, it is important that the fluorescence intensities of the QDs remain unaffected by the pH value.[43] For our method, GSH-capped

DOI: 10.1021/acsami.5b05503
ACS Appl. Mater. Interfaces 2015, 7, 17623−17629

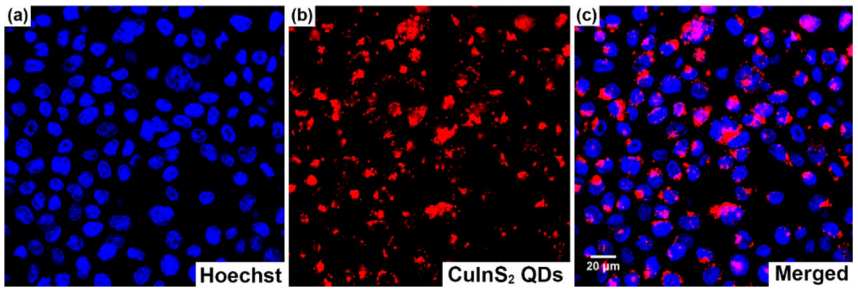

Figure 6. Cell confocal images of Hoechst dyed nucleus (a), $CuInS_2$ QDs (b), and merged image (c).

QDs in phosphate buffer solution (PBS) of pH value between 2 and 13 were determined by measuring the PL intensity after 5 h (see Figure 5b and Figure S6 in the Supporting Information). We also determined the stability of these samples under different temperature and light exposure (see Figure S7 in the Supporting Information). These results show that the QDs transferred by this method can be stable between 4 and 12, implying the potential application for sensor and detection.

To demonstrate the potential bioimaging application, we first determined the cytotoxicity of GSH-capped $CuInS_2$/ZnS QDs. As shown in Figure S8 in the Supprorting Information, no significant cytotoxicity was observed for the doses that we used here. We then carried out the cell confocal imaging to verify the imaging applications of GSH-capped $CuInS_2$/ZnS QDs (see Figure 6). In Figure 6a, MCF10CA1a breast tumor cells were stained with Hoechst (blue), while the red color in Figure 6b is from $CuInS_2$/ZnS QDs. It is obviously that the $CuInS_2$/ZnS QDs can enter and successfully image the cells. Notably, most of the $CuInS_2$/ZnS QDs were in the cytoplasm. Some were in the perinuclear area. These results demonstrate the potential for further application of the QDs in bioimaging and diagnosis. More related works are currently underway.

4. CONCLUSION

The aqueous phase transfer of $CuInS_2$/ZnS QDs was achieved through an efficient ligand exchange strategy using GSH as the bifunctional ligand. According to the experiment phenomena and characterization results, MPA is an essential additive for GSH ligand exchanging. TEM and DLS results show that there is no obvious change in the particle size and monodispersity of QDs during the ligand exchange process. Meanwhile, the fluorescent of hydrophilic $CuInS_2$/ZnS QDs can maintain a PLQY of 34%, which is almost ~50% of hydrophobic $CuInS_2$/ZnS QDs. Most importantly, the stability of aqueous solution of $CuInS_2$/ZnS QDs is marvelous. The aqueous solution can be stored at 4 °C for nearly three months without any aggregation or fluorescent quenching. In conclusion, the small particle size, good fluorescent intensity and impressed stability make GSH-capped $CuInS_2$/ZnS QDs promising candidates for optical bioimaging, especially in cell imaging. Particularly, the versatility of this ligand exchange strategy for colloidal quantum dots was demonstrated by extending it to the aqueous transferring of other hydrophobic quantum dots, for instance, $CuInSe_2$ and CdSe/ZnS quantum dots. We believed that the available gram-scale GSH-capped QDs also have the opportunities to promote the applications in other fields such as photocatalysis,[67] QDs-sensitized solar cells,[68] etc.

■ ASSOCIATED CONTENT

Supporting Information

The Supporting Information is available free of charge on the ACS Publications website at DOI: 10.1021/acsami.5b05503.

Experimental details concerning other methods of phase transfer. Results of experiments with different ratio of GSH and MPA. UV and PL spectra, optical picture of the sample, and thermogravimetric analysis. Stability test with different pH and temperatures, under daylight and UV light and the results of the MTT test. (PDF)

■ AUTHOR INFORMATION

Corresponding Author

*E-mail: hzzhong@bit.edu.cn. Fax: +86-10-68918188. Tel: +86-10-68918188.

Author Contributions

∥The manuscript was written through contributions of all authors. All authors have given approval to the final version of the manuscript. These authors contributed equally.

Notes

The authors declare no competing financial interest.

■ ACKNOWLEDGMENTS

The authors would like to thanks the funding support of the National Basic Research Program of China (2011CB933600), National Natural Science Foundation of China (21343005), Beijing Higher Education Young Elite Teacher Project (YETP1231), and the Open Research Fund of State Key Laboratory of Bioelectronics Southeast University. The authors would like to thanks Prof. Hai-Yan Xie, Dr. Andrew Wang, Prof. Yi Lin, and Prof. Zengguo Feng for the optical measurements, helpful discussions, and manuscript comments.

■ REFERENCES

(1) Chan, W. C. W.; Nie, S. M. Quantum Dot Bioconjugates for Ultrasensitive Nonisotopic Detection. *Science* **1998**, *281*, 2016−2018.
(2) Medintz, I. L.; Uyeda, H. T.; Goldman, E. R.; Mattoussi, H. Quantum Dot Bioconjugates for Imaging, Labelling and Sensing. *Nat. Mater.* **2005**, *4*, 435−446.
(3) Michalet, X.; Pinaud, F. F.; Bentolila, L. A.; Tsay, J. M.; Doose, S.; Li, J. J.; Sundaresan, G.; Wu, A. M.; Gambhir, S. S.; Weiss, S. Quantum Dots for Live Cells, *In vivo* Imaging, and Diagnostics. *Science* **2005**, *307*, 538−544.
(4) Li, Z.; Sun, Q.; Zhu, Y.; Tan, B.; Xu, Z. P.; Dou, S. X. Ultra-small Fluorescent Inorganic Nanoparticles for Bio-imaging. *J. Mater. Chem. B* **2014**, *2*, 2793−2818.
(5) Biju, V.; Itoh, T.; Ishikawa, M. Delivering Quantum Dots to Cells: Bioconjugated Quantum Dots for Targeted and Nonspecific Extracellular and Intracellular Imaging. *Chem. Soc. Rev.* **2010**, *39*, 3031−3056.

DOI: 10.1021/acsami.5b05503
ACS Appl. Mater. Interfaces 2015, 7, 17623−17629

(6) Wu, X.; Liu, H.; Liu, J.; Haley, K. N.; Treadway, J. A.; Larson, J. P.; Ge, N. F.; Peale, F.; Bruchez, M. P. Immunofluorescent Labeling of Cancer Marker Her2 and Other Cellular Targets with Semiconductor Quantum Dots. *Nat. Biotechnol.* **2002**, *21*, 41−46.
(7) Kim, S.; Bawendi, M. G. Oligomeric Ligands for Luminescent and Stable Nanocrystal Quantum Dots. *J. Am. Chem. Soc.* **2003**, *125*, 14652−14653.
(8) Li, Y. L.; Jing, L. H.; Qiao, R. R.; Gao, M. Y. Aqueous Synthesis of CdTe Nanocrystals: Progresses and Perspectives. *Chem. Commun.* **2011**, *47*, 9293−9311.
(9) Howes, P. D.; Chandrawati, R.; Stevens, M. M. Colloidal Nanoparticles as Advanced Biological Sensors. *Science* **2014**, *346*, 53−63.
(10) Li, J. J.; Zhu, J. J. Quantum Dots for Fluorescent Biosensing and Bio-imaging Applications. *Analyst* **2013**, *138*, 2506−2515.
(11) Ma, Q.; Lin, Z. H.; Yang, N.; Li, Y.; Su, X. G. A Novel Carboxymethyl Chitosan−Quantum Dot-Based Intracellular Probe for Zn^{2+} Ion Sensing in Prostate Cancer Cells. *Acta Biomater.* **2014**, *10*, 868−874.
(12) Smith, A. M.; Duan, H.; Mohs, A. M.; Nie, S. M. Bioconjugated Quantum Dots for *In vivo* Molecular and Cellular Imaging. *Adv. Drug Delivery Rev.* **2008**, *60*, 1226−1240.
(13) Cassette, E.; Helle, M.; Bezdetnaya, L.; Marchal, F.; Dubertret, B.; Pons, T. Design of New Quantum Dot Materials for Deep Tissue Infrared Imaging. *Adv. Drug Delivery Rev.* **2013**, *65*, 719−731.
(14) Zhong, H. Z.; Bai, Z. L.; Zou, B. S. Tuning the Luminescence Properties of Colloidal I−III−VI Semiconductor Nanocrystals for Optoelectronics and Biotechnology Applications. *J. Phys. Chem. Lett.* **2012**, *3*, 3167−3175.
(15) Kolny-Olesiak, J.; Weller, H. Synthesis and Application of Colloidal $CuInS_2$ Semiconductor Nanocrystals. *ACS Appl. Mater. Interfaces* **2013**, *5*, 12221−12237.
(16) Aldakov, D.; Lefrancois, A.; Reiss, P. Ternary and Quaternary Metal Chalcogenide Nanocrystals: Synthesis, Properties and Applications. *J. Mater. Chem. C* **2013**, *1*, 3756−3776.
(17) Deng, D. W.; Chen, Y. Q.; Cao, J.; Tian, J. M.; Qian, Z. Y.; Achilefu, S.; Gu, Y. Q. High-Quality $CuInS_2$/ZnS Quantum Dots for *In vitro* and *In vivo* Bio-imaging. *Chem. Mater.* **2012**, *24*, 3029−3037.
(18) Yu, K.; Ng, P.; Ouyang, J.; Zaman, M. B.; Abulrob, A.; Baral, T. N.; Fatehi, D.; Jakubek, Z. J.; Kingston, D.; Wu, X. H.; Liu, X. Y.; Hebert, C.; Leek, D. M.; Whitfield, D. M. Low-Temperature Approach to Highly Emissive Copper Indium Sulfide Colloidal Nanocrystals and Their Bio-imaging Applications. *ACS Appl. Mater. Interfaces* **2013**, *5*, 2870−2880.
(19) Lin, Z. H.; Fei, X. F.; Ma, Q.; Gao, X.; Su, X. G. $CuInS_2$ Quantum Dots@Silica Near-Infrared Fluorescent Nanoprobe for Cell Imaging. *New J. Chem.* **2014**, *38*, 90−96.
(20) Liu, S. Y.; Su, X. G. The Synthesis and Application of I−III−VI Type Quantum Dots. *RSC Adv.* **2014**, *4*, 43415−43428.
(21) Liu, S.; Zhang, H.; Qiao, Y.; Su, X. G. One-pot Synthesis of Ternary $CuInS_2$ Quantum Dots with Near-Infrared Fluorescence in Aqueous Solution. *RSC Adv.* **2012**, *2*, 819−825.
(22) Guo, W. S.; Chen, N.; Dong, C.; Tu, Y.; Chang, J.; Zhang, B. B. One-Pot Synthesis of Hydrophilic ZnCuInS/ZnS Quantum Dots for *In vivo* Imaging. *RSC Adv.* **2013**, *3*, 9470−9475.
(23) Chen, Y. Y.; Li, S. J.; Huang, L. J.; Pan, D. C. Green and Facile Synthesis of Water-Soluble Cu−In−S/ZnS Core/Shell Quantum Dots. *Inorg. Chem.* **2013**, *52*, 7819−7821.
(24) Chen, B. K.; Zhong, H. Z.; Zhang, W. Q.; Tan, Z. A.; Li, Y. F.; Yu, C. R.; Zhai, T. Y.; Bando, Y.; Yang, S. Y.; Zou, B. S. Highly Emissive and Color-Tunable $CuInS_2$-Based Colloidal Semiconductor Nanocrystals: Off-Stoichiometry Effects and Improved Electroluminescence Performance. *Adv. Funct. Mater.* **2012**, *22*, 2081−2088.
(25) Li, L.; Daou, T. J.; Texier, I.; Tran, T. K. C.; Nguyen, Q. L.; Reiss, P. Highly Luminescent $CuInS_2$/ZnS Core/Shell Nanocrystals: Cadmium-Free Quantum Dots for *In vivo* Imaging. *Chem. Mater.* **2009**, *21*, 2422−2429.
(26) Tang, X. S.; Cheng, W. L.; Choo, E. S. G.; Xue, J. Synthesis of $CuInS_2$−ZnS Alloyed Nanocubes with High Luminescence. *Chem. Commun.* **2011**, *47*, 5217−5219.
(27) Zhang, J.; Xie, R. G.; Yang, W. S. A Simple Route for Highly Luminescent Quaternary Cu-Zn-In-S Nanocrystal Emitters. *Chem. Mater.* **2011**, *23*, 3357−3361.
(28) Zhang, W. J.; Zhong, X. H. Facile Synthesis of ZnS-$CuInS_2$-Alloyed Nanocrystals for a Color-Tunable Fluorchrome and Photocatalyst. *Inorg. Chem.* **2011**, *50*, 4065−4072.
(29) Pons, T.; Pic, E.; Lequeux, N.; Cassette, E.; Bezdetnaya, L.; Guillemin, F.; Marchal, F.; Dubertret, B. Cadmium-Free $CuInS_2$/ZnS Quantum Dots for Sentinel Lymph Node Imaging with Reduced Toxicity. *ACS Nano* **2010**, *4*, 2531−2538.
(30) Speranskaya, E. S.; Beloglazova, N. V.; Abe, S.; Aubert, T.; Smet, P. F.; Poelman, D.; Goryacheva, I. Y.; De Saeger, S.; Hens, Z. Hydrophilic, Bright $CuInS_2$ Quantum Dots as Cd-Free Fluorescent Labels in Quantitative Immunoassay. *Langmuir* **2014**, *30*, 7567−7575.
(31) Sun, X.; Ding, K.; Hou, Y.; Gao, Z.; Yang, W.; Jing, L.; Gao, M. Y. Bifunctional Superparticles Achieved by Assembling Fluorescent $CuInS_2$@ZnS Quantum Dots and Amphibious Fe_3O_4 Nanocrystals. *J. Phys. Chem. C* **2013**, *117*, 21014−21020.
(32) Yong, K. T.; Roy, I.; Hu, R.; Ding, H.; Cai, H. X.; Zhu, J.; Zhang, X. H.; Bergey, E. J.; Prasad, P. N. Synthesis of Ternary $CuInS_2$/ZnS Quantum Dot Bioconjugates and Their Applications for Targeted Cancer Bio-imaging. *Integr. Biol.* **2010**, *2*, 121−129.
(33) Deng, D. W.; Chen, Y. Q.; Cao, J. M.; Tian, J. M.; Qian, Z. Y.; Achilefu, S.; Gu, Y. Q. High-Quality $CuInS_2$/ZnS Quantum Dots for *In vitro* and *In vivo* Bio-imaging. *Chem. Mater.* **2012**, *24*, 3029−3037.
(34) Cassette, E.; Pons, T.; Bouet, C.; Helle, M.; Bezdetnaya, L.; Marchal, F.; Dubertret, B. Synthesis and Characterization of Near-Infrared Cu−In−Se/ZnS Core/Shell Quantum Dots for *In vivo* Imaging. *Chem. Mater.* **2010**, *22*, 6117−6124.
(35) Lesnyak, V.; Gaponik, N.; Eychmüller, A. Colloidal Semiconductor Nanocrystals: The Aqueous Approach. *Chem. Soc. Rev.* **2013**, *42*, 2905−2929.
(36) Zhang, P. F.; Liu, S. H.; Gao, D. Y.; Hu, D. H.; Gong, P.; Sheng, Z. H.; Deng, J. Z.; Ma, Y. F.; Cai, L. T. Click-Functionalized Compact Quantum Dots Protected by Multidentate-Imidazole Ligands: Conjugation-Ready Nanotags for Living-Virus Labeling and Imaging. *J. Am. Chem. Soc.* **2012**, *134*, 8388−8391.
(37) Finetti, C.; Colombo, M.; Prosperi, D.; Alessio, G.; Morasso, C.; Sola, L.; Chiari, M. One-Pot Phase Transfer and Surface Modification of CdSe-ZnS Quantum Dots Using a Synthetic Functional Copolymer. *Chem. Commun.* **2014**, *50*, 240−242.
(38) Dai, M. Q.; Yung, L. Y. L. Ethylenediamine-Assisted Ligand Exchange and Phase Transfer of Oleophilic Quantum Dots: Stripping of Original Ligands and Preservation of Photoluminescence. *Chem. Mater.* **2013**, *25*, 2193−2201.
(39) Howarth, M.; Takao, K.; Hayashi, Y.; Ting, A. Y. Targeting Quantum Dots to Surface Proteins in Living Cells with Biotin Ligase. *Proc. Natl. Acad. Sci. U. S. A.* **2005**, *102*, 7583−7588.
(40) Jing, L.; Yang, C.; Qiao, R.; Niu, M.; Du, M.; Wang, D.; Gao, M. Highly Fluorescent CdTe@SiO_2 Particles Prepared via Reverse Microemulsion Method. *Chem. Mater.* **2010**, *22*, 420−427.
(41) Guo, W. S.; Chen, N.; Tu, Y.; Dong, C. H.; Zhang, B. B.; Hu, C. H.; Chang, J. Synthesis of Zn-Cu-In-S/ZnS Core/Shell Quantum Dots with Inhibited Blue-Shift Photoluminescence and Applications for Tumor Targeted Bio-imaging. *Theranostics* **2013**, *3*, 99−108.
(42) Pathak, S.; Choi, S. K.; Arnheim, N.; Thompson, M. E. Hydroxylated Quantum Dots as Luminescent Probes for *In Situ* Hybridization. *J. Am. Chem. Soc.* **2001**, *123*, 4103−4104.
(43) Pong, B. K.; Trout, B. L.; Lee, J. Y. Modified Ligand-Exchange for Efficient Solubilization of CdSe/ZnS Quantum Dots in Water: A Procedure Guided by Computational Studies. *Langmuir* **2008**, *24*, 5270−5276.
(44) Durán, G. M.; Plata, M. R.; Zougagh, M.; Contento, A. M.; Ríos, Á. Microwave-Assisted Synthesis of Water Soluble Thiol Capped CdSe/ZnS Quantum Dots and Its Interaction with Sulfonylurea Herbicides. *J. Colloid Interface Sci.* **2014**, *428*, 235−241.

DOI: 10.1021/acsami.5b05503
ACS Appl. Mater. Interfaces 2015, 7, 17623−17629

(45) Aldana, J.; Wang, Y. A.; Peng, X. G. Photochemical Instability of CdSe Nanocrystals Coated by Hydrophilic Thiols. *J. Am. Chem. Soc.* **2001**, *123*, 8844−8850.
(46) Tamang, S.; Beaune, G.; Texier, I.; Reiss, P. Aqueous Phase Transfer of InP/ZnS Nanocrystals Conserving Fluorescence and High Colloidal Stability. *ACS Nano* **2011**, *5*, 9392−9402.
(47) Wang, Y. A.; Li, J. J.; Chen, H. Y.; Peng, X. G. Stabilization of Inorganic Nanocrystals by Organic Dendrons. *J. Am. Chem. Soc.* **2002**, *124*, 2293−2298.
(48) Susumu, K.; Uyeda, H. T.; Medintz, I. L.; Pons, T.; Delehanty, J. B.; Mattoussi, H. Enhancing the Stability and Biological Functionalities of Quantum Dots via Compact Multifunctional Ligands. *J. Am. Chem. Soc.* **2007**, *129*, 13987−13996.
(49) Zhang, L. M.; Lu, Z. X.; Bai, Y. Y.; Wang, T.; Wang, Z. F.; Chen, J.; Ding, Y.; Yang, F.; Xiao, Z. D.; Ju, S.; Zhu, J. J.; He, N. Y. PEGylated Denatured Bovine Serum Albumin Modified Water-Soluble Inorganic Nanocrystals as Multifunctional Drug Delivery Platforms. *J. Mater. Chem. B* **2013**, *1*, 1289−1295.
(50) Rodrigues, S. S. M.; Ribeiro, D. S. M.; Molina-Garcia, L.; Medina, A. R.; Prior, J. A. V.; Santos, J. L. M. Fluorescence Enhancement of CdTe MPA-Capped Quantum Dots by Glutathione for Hydrogen Peroxide Determination. *Talanta* **2014**, *122*, 157−165.
(51) Li, Y. Y.; Zhou, Y. L.; Wang, H. Y.; Perrett, S.; Zhao, Y. L.; Tang, Z. Y.; Xie, G. J. Chirality of Glutathione Surface Coating Affects the Cytotoxicity of Quantum Dots. *Angew. Chem., Int. Ed.* **2011**, *50*, 5860−5864.
(52) Baumle, M.; Stamou, D.; Segura, J. M.; Hovius, R.; Vogel, H. Highly Fluorescent Streptavidin-Coated CdSe Nanoparticles: Preparation in Water, Characterization, and Micropatterning. *Langmuir* **2004**, *20*, 3828−3831.
(53) Samanta, A.; Deng, Z. T.; Liu, Y. Aqueous Synthesis of Glutathione-Capped CdTe/CdS/ZnS and CdTe/CdSe/ZnS Core/Shell/Shell Nanocrystal Heterostructures. *Langmuir* **2012**, *28*, 8205−8215.
(54) Zheng, Y. G.; Yang, Z. C.; Ying, J. Y. Aqueous Synthesis of Glutathione-Capped ZnSe and $Zn_{1-x}Cd_xSe$ Alloyed Quantum Dots. *Adv. Mater.* **2007**, *19*, 1475−1479.
(55) Cui, R.; Liu, H. H.; Xie, H. Y.; Zhang, Z. L.; Yang, Y. R.; Pang, D. W.; Xie, Z. X.; Chen, B. B.; Hu, B.; Shen, P. Living Yeast Cells as a Controllable Biosynthesizer for Fluorescent Quantum Dots. *Adv. Funct. Mater.* **2009**, *19*, 2359−2364.
(56) Zhong, H. Z.; Zhou, Y.; Ye, M. F.; He, Y. J.; Ye, J. P.; He, C.; Yang, C. H.; Li, Y. F. Controlled Synthesis and Optical Properties of Colloidal Ternary Chalcogenide $CuInS_2$ Nanocrystals. *Chem. Mater.* **2008**, *20*, 6434−6443.
(57) Zhong, H. Z.; Lo, S. S.; Mirkovic, T.; Li, Y. C.; Ding, Y. Q.; Li, Y. F.; Scholes, G. D. Noninjection Gram-scale Synthesis of Monodisperse Pyramidal $CuInS_2$ Nanocrystals and Their Size-Dependent Properties. *ACS Nano* **2010**, *4*, 5253−5262.
(58) Zhong, H. Z.; Wang, Z. B.; Bovero, E.; Lu, Z. H.; Veggel, F. C. J.; Scholes, G. D. Colloidal $CuInSe_2$ Nanocrystals in The Quantum Confinement Regime: Synthesis, Optical Properties, and Electroluminescence. *J. Phys. Chem. C* **2011**, *115*, 12396−12402.
(59) Crosby, G. A.; Demas, J. N. Measurement of Photoluminescence Quantum Yields. Review. *J. Phys. Chem.* **1971**, *75*, 991−1024.
(60) Liu, X. Y.; Wei, W.; Wang, C. L.; Yue, H.; Ma, D.; Zhu, C.; Ma, G. H.; Du, Y. G. Apoferritin-Camouflaged Pt Nanoparticles: Surface Effects on Cellular Uptake and Cytotoxicity. *J. Mater. Chem.* **2011**, *21*, 7105−7110.
(61) Millis, K. K.; Weaver, K. H.; Rabenstein, D. L. Oxidation/Reduction Potendial of Gllutathione. *J. Org. Chem.* **1993**, *58*, 4144−4146.
(62) Santra, S.; Yang, H.; Holloway, P. H.; Stanley, J. T.; Mericle, R. A. Synthesis of Water-Dispersible Fluorescent, Radio-Opaque, and Paramagnetic CdS:Mn/ZnS Quantum Dots: A Multifunctional Probe for Bio-imaging. *J. Am. Chem. Soc.* **2005**, *127*, 1656−1657.
(63) Wang, M. N.; Liu, X. Y.; Cao, C. B.; Wang, L. Highly Luminescent $CuInS_2$-ZnS Nanocrystals: Achieving Phase Transfer and Nuclear Homing Property Simultaneously Through Simple TTAB Modification. *J. Mater. Chem.* **2012**, *22*, 21979−21986.
(64) Algar, W. R.; Krull, U. J. Luminescence and Stability of Aqueous Thioalkyl Acid Capped CdSe/ZnS Quantum Dots Correlated to Ligand Ionization. *ChemPhysChem* **2007**, *8*, 561−568.
(65) Coto-García, A. M.; Fernández-Argüelles, M. T.; Costa-Fernández, J. M.; Sanz-Medel, A.; Valledor, M.; Campo, J. C.; Ferrero, F. J. The Influence of Surface Coating on the Properties of Water-Soluble CdSe and CdSe/ZnS Quantum Dots. *J. Nanopart. Res.* **2013**, *15*, 1−11.
(66) Chen, C. W.; Wu, D. Y.; Chan, Y. C.; Lin, C. C.; Chung, P. H.; Hsiao, M.; Liu, R. S. Evaluations of the Chemical Stability and Cytotoxicity of $CuInS_2$ and $CuInS_2$/ZnS Core/Shell Quantum Dots. *J. Phys. Chem. C* **2015**, *119*, 2852−2860.
(67) Han, Z. J.; Qiu, F.; Eisenberg, R.; Holland, P. L.; Krauss, T. D. Robust Photogeneration of H-2 in Water Using Semiconductor Nanocrystals and a Nickel Catalyst. *Science* **2012**, *338*, 1321−1324.
(68) Pan, Z. X.; Mora-Seró, I.; Shen, Q.; Zhang, H.; Li, Y.; Zhao, K.; Wang, J.; Zhong, X. H.; Bisquert, J. High-Efficiency "Green" Quantum Dot Solar Cells. *J. Am. Chem. Soc.* **2014**, *136*, 9203−9210.

DOI: 10.1021/acsami.5b05503
ACS Appl. Mater. Interfaces 2015, 7, 17623−17629